Supporting Information for

A Triangular Platinum(II) Multi-nuclear Complex with Cytotoxicity Towards Breast Cancer Stem Cells

Arvin Eskandari,[a] Arunangshu Kundu,[b] Sushobhan Ghosh,[b]* and Kogularamanan Suntharalingam[c]*

[a] Department of Chemistry, King's College London, London, UK
[b] Department of Chemistry, Gauhati University, Guwahati, India
[c] Department of Chemistry, University of Leicester, Leicester, UK

* To whom correspondence should be addressed:
Email: kogularamanan.suntharalingam@kcl.ac.uk and sushobhan.iisc@gmail.com

Table of Content

Experimental Details

Experimental Details

Materials and Methods. All synthetic procedures were performed under normal atmospheric conditions or under nitrogen. Fourier transform infrared (FTIR) spectra were recorded with an IRAffinity-1S Shimadzu spectrophotometer. High resolution electron spray ionisation mass spectra were recorded on a BrukerDaltronics Esquire 3000 spectrometer by Dr. Lisa Haigh (Imperial College London). UV-Vis absorption spectra were recorded on a Cary100 UV-Vis spectrophotometer. ^{1}H NMR spectra were recorded on a BrukerAvance 400 MHz Ultrashield NMR spectrometer. ^{1}H NMR spectra were referenced internally to residual solvent peaks, and chemical shifts are expressed relative to tetramethylsilane, $SiMe_4$ ($\delta = 0$ ppm). Elemental analysis of the compounds prepared was performed commercially by London Metropolitan University. The platinum(II) complexes **Pt-1a** and **Pt-1b** was prepared according to a previously reported protocol.[1] Benzotriazole and sodium methoxide were purchased from Sigma Aldrich and used as received. For all biological studies, the concentrations of **Pt-1**, **Pt-2**, and **Pt-3** were based on platinum concentration.

Synthesis of the tri-nuclear platinum(II) complex, Pt-3. To a dry DMF solution (5 mL) containing benzotriazole (11.9 mg, 0.1 mmol) and sodium methoxide (5.4 mg, 0.1 mmol), a dry DMF solution (5 mL) containing **Pt-1a** (89.1 mg, 0.1 mmol) was added. The resultant pale yellow mixture was stirred at 80°C for 3 h. The solution was then reduced and methanol was added to give a DMF:methanol (1:9) ratio. The resulting solution was centrifuged. The clear centrifugate was collected and treated with diethyl ether to obtain **Pt-3** as a colourless solid (229 mg, 88%); ^{1}H NMR (400 MHz, DMSO-d_6) δ_H 8.21 (dd, 10H), 7.65 (t, 6H), 7.58-7.46 (m, 16H), 7.32 (t, 6H), 7.20 (br s, 4H), 6.69-6.87 (m, 20H), 6.74 (dd, 5H), 6.33 (dd, 5H), 3.66-3.52 (m, 6H), 2.61-2.53 (m, 6H); IR (solid, cm^{-1}): 1650, 1487, 1437, 1258, 1225, 1152, 1107, 1029, 995, 883, 816, 777, 749, 721, 704, 693, 637; ESI-MS Calcd. for $C_{96}H_{84}N_9P_6Pt_3$ $[M\text{-}3SO_3CF_3]^{3+}$: 711.2554 a.m.u. Found $[M\text{-}3SO_3CF_3]^{3+}$: 711.4751 a.m.u., Calcd. for $C_{97}H_{84}F_3N_9O_3P_6Pt_3S$ $[M\text{-}2SO_3CF_3]^{2+}$: 1141.1850 a.m.u. Found $[M\text{-}2SO_3CF_3]^{2+}$: 1141.7004. Anal. Calcd. for $C_{99}H_{84}F_9N_9O_9P_6Pt_3S_3$•DMF : C, 46.16; H, 3.42; N, 5.28. Found: C, 46.38; H, 3.64; N, 5.03.

Characterisation discussion for the tri-nuclear platinum(II) complex, Pt-3. The IR spectrum of **Pt-3** lacked a broad signal in the 3500-3350 cm^{-1} region corresponding to the N-H functional group found in benzotriazole (Figure S3). This suggests that the benzotriazole ligands in **Pt-3** are deprotonated and bind to platinum via the nitrogen atoms (as depicted in Scheme S1). Distinctive molecular ion peaks corresponding to [**Pt-3**-$2SO_3CF_3]^{2+}$ (1141.7004 m/z) and [**Pt-3**-$3SO_3CF_3]^{3+}$ (711.4751 m/z) with the appropriate isotopic distribution was observed in the positive mode of the ESI mass spectrum (Figure S4).

Synthesis of the di-nuclear platinum(II) complex, Pt-2. To a dry DMF solution (5 mL) containing benzotriazole (11.9 mg, 0.1 mmol) and sodium methoxide (5.4 mg, 0.1 mmol), a dry DMF solution (5 mL) containing **Pt-1b** (178.2 mg, 0.2 mmol) was added. The resultant pale yellow mixture was stirred at 80°C for 3 h. The solution was then reduced and DCM was added to give a DMF:DCM (1:9) ratio. The resulting solution was centrifuged. The clear centrifugate was collected and treated with diethyl ether to obtain **Pt-3** as a colourless solid (116 mg, 82%); IR (solid, cm^{-1}): 1649, 1487, 1442, 1257, 1224, 1157, 1106, 1028, 1000, 882, 827, 776, 748, 720, 704, 692, 636, 575, 536; ESI-MS Calcd. for $C_{58}H_{52}Cl_2N_3P_4Pt_2$ $[M\text{-}Cl]^+$: 1375.3763 a.m.u. Found $[M\text{-}Cl]^+$: 1375.1796 a.m.u.; Anal. Calcd. for $C_{58}H_{52}Cl_3N_3P_4Pt_2$: C, 49.35; H, 3.71; N, 2.98. Found: C, 49.55; H, 3.62; N, 3.12.

Characterisation discussion for the di-nuclear platinum(II) complex, Pt-2. Similarly to **Pt-3,** the IR spectrum of **Pt-2** did not display a N-H stretch (Figure S3), implying that the benzotriazole ligand in **Pt-2** is deprotonated and binds to platinum via the nitrogen atoms (as depicted in Scheme S2). A distinctive molecular ion peak corresponding to [**Pt-2**-Cl]$^+$ (1375.1796 m/z) with the appropriate isotopic distribution was observed in the positive mode of the ESI mass spectrum (Figure S5).

X-ray Single Crystal Diffraction Analysis. Standard procedures were used to mount the crystal on a Gemini diffractometer with graphite-monochromated Mo Kα radiation (λ = 0.71073 Å) at 293 K. The crystal structure was solved using direct methods in SHELXS and refined by full-matrix least-squares routines, based on F^2, using the SHELXL program.[2] All the H atoms were placed in geometrically idealised positions and constrained to ride on their parent atoms. The structure has been deposited with the Cambridge Crystallographic Data Centre (CCDC 1906805 and 1906803). This information can be obtained free of charge from

Cell Lines and Cell Culture Conditions. The human mammary epithelial cell lines, HMLER and HMLER-shEcad were kindly donated by Prof. R. A. Weinberg (Whitehead Institute, MIT). The human epithelial breast MCF710A cell line was acquired from the American Type Culture Collection (ATCC, Manassas, VA, USA). HMLER, HMLER-shEcad, and MCF10A cells were maintained in Mammary Epithelial Cell Growth Medium (MEGM) with supplements and growth factors (BPE, hydrocortisone, hEGF, insulin, and gentamicin/amphotericin-B). The cells were grown at 310 K in a humidified atmosphere containing 5% CO_2.

Cytotoxicity MTT assay. The colourimetric MTT assay was used to determine the toxicity of **Pt-1a**, **Pt-2**, **Pt-3**, cisplatin, carboplatin, and salinomycin. HMLER, HMLER-shEcad, and MCF10A cells (5×10^3) were seeded in each well of a 96-well plate. After incubating the cells overnight, various concentrations of the compounds (0.2-100 μM), were added and incubated for 72 h (total volume 200 μL). Stock solutions of the compounds were prepared as 10 mM solutions in DMSO and diluted using media. The final concentration of DMSO in each well was 0.5% and this amount was present in the untreated control as well. After 72 h, 20 μL of a 4 mg/mL solution of MTT in PBS was added to each well, and the plate was incubated for an additional 4 h. The MEGM/MTT mixture was aspirated and 200 μL of DMSO was added to dissolve the resulting purple formazan crystals. The absorbance of the solutions in each well was read at 550 nm. Absorbance values were normalized to (DMSO-containing) control wells and plotted as concentration of test compound versus % cell viability. IC_{50} values were interpolated from the resulting dose dependent curves. The reported IC_{50} values are the average of three independent experiments, each consisting of six replicates per concentration level (overall n = 18).

Tumorsphere Formation and Viability Assay. HMLER-shEcad cells (5×10^3) were plated in ultralow-attachment 96-well plates (Corning) and incubated in MEGM supplemented with B27 (Invitrogen), 20 ng/mL EGF, and 4 μg/mL heparin (Sigma) for 5 days. Studies were also conducted in the presence of **Pt-1a**, **Pt-2**, **Pt-3**, cisplatin, and carboplatin (0-133 μM). Mammospheres treated with **Pt-1a**, **Pt-2**, **Pt-3**, cisplatin, carboplatin, and salinomycin (at their respective IC_{20} values, 5 days) were counted and imaged using an inverted microscope. The viability of the mammospheres was determined by addition of a resazurin-based reagent, TOX8 (Sigma). After incubation for 16 h, the solutions were carefully transferred to a black 96-well plate (Corning), and the fluorescence of the solutions was read at 590 nm (λ_{ex} = 560 nm). Viable mammospheres reduce the amount of the oxidized TOX8 form (blue) and

concurrently increases the amount of the fluorescent TOX8 intermediate (red), indicating the degree of mammosphere cytotoxicity caused by the test compound. Fluorescence values were normalized to DMSO-containing controls and plotted as concentration of test compound versus % mammospheres viability. IC_{50} values were interpolated from the resulting dose dependent curves. The reported IC_{50} values are the average of two independent experiments, each consisting of three replicates per concentration level (overall n = 6).

Cellular Uptake. To measure the cellular uptake of **Pt-2**, **Pt-3**, and cisplatin *ca.* 1 million HMLER-shEcad cells were treated with **Pt-2**, **Pt-3**, and cisplatin (2 μM) at 37 ºC for 24 h. After incubation, the media was removed and the cells were washed with PBS (2 mL × 3), and harvested. The number of cells was counted at this stage, using a haemocytometer. This mitigates any cell death induced by **Pt-2**, **Pt-3**, and cisplatin at the administered concentration and experimental cell loss. The cells were centrifuged to form pellets. The cellular pellets were dissolved in 65% HNO_3 (250 μL) overnight. The cellular pellets were also used to determine the platinum content in the nuclear fraction. The Thermo Scientific NE-PER Nuclear and Cytoplasmic Extraction Kit was used to extract and separate the nuclear, fraction. The fractions were dissolved in 65% HNO_3 overnight (250 μL final volume). All samples were diluted 5-fold with water and analysed using inductively coupled plasma mass spectrometry (ICP-MS, PerkinElmer NexION 350D). Platinum levels are expressed as Pt (ppb) per million cells. Results are presented as the mean of five determinations for each data point.

Measurement of water-octanol partition coefficient (LogP). The LogP value for **Pt-2** and **Pt-3** was determined using the shake-flask method and UV-Vis spectroscopy. The octanol used in this experiment was pre-saturated with water. An aqueous solution of **Pt-2** and **Pt-3** (500 μL, 100 μM) was incubated with octanol (500 μL) in a 1.5 mL tube. The tube was shaken at room temperature for 24 h. The two phases were separated by centrifugation and the **Pt-2** and **Pt-3** content in each phase was determined by UV-Vis spectroscopy.

Immunoblotting Analysis. HMLER-shEcad cells (5×10^3 cells) were incubated with **Pt-3** (at various concentrations, 0.5, 1, and 2 μM) for 72 h at 37 ºC. Cells were washed with PBS, scraped into SDS-PAGE loading buffer (64 mM Tris-HCl (pH6.8)/ 9.6% glycerol/ 2%SDS/ 5% β-mercaptoethanol/ 0.01% Bromophenol Blue), and incubated at 95 ºC for 10 min. Whole cell lysates were resolved by 4-20 % sodium dodecylsulphate polyacylamide gel electrophoresis (SDS-PAGE; 200 V for 25 min) followed by electro transfer to polyvinylidene difluoride membrane, PVDF (350 mA for 1 h). Membranes were blocked in 5% (w/v) non-fat milk in PBST (PBS/0.1% Tween 20) and incubated with the appropriate primary antibodies (Cell Signalling Technology). After incubation with horseradish peroxidase-conjugated secondary antibodies (Cell Signalling Technology), immune complexes were detected with the ECL detection reagent (BioRad) and analysed using a chemiluminescence imager (Amersham Imager 600).

ct-DNA precipitation assay. A solution of ct-DNA (0.25 mM, nucleotide) was incubated with **Pt-3**, **Pt-2**, or cisplatin at a base pair:platinum ratio of 5:1 at 37 ºC in PBS at 37 ºC. After 4 h incubation, a 250 μL aliquot was removed and the DNA was precipitated by adding 10 μL of KCl (5 M) and 1 mL of EtOH (stored at 4 °C). The solution was centrifuged at 4 °C to isolate the DNA. The isolated DNA samples were dissolved in 65% HNO_3 overnight (250 μL final volume). All samples were diluted 5-fold with water and analysed using inductively coupled plasma mass spectrometry (ICP-MS, PerkinElmer NexION 350D). Platinum levels were expressed as mg/L, and corresponded to the concentration of covalently bound **Pt-3**, **Pt-**

2, or cisplatin on DNA. Results are presented as the mean of five determinations for each data point.

Ethidium Bromide and DAPI Displacement Studies. To a mixture of ethidium bromide (1 µM) or DAPI (1 µM), and ct-DNA (20 µM) in 5 mM Tris–HCl (pH 7.4) buffer an increasing amount of the platinum(II) complexes, **Pt-1a**, **Pt-2**, and **Pt-3** (0-35 µM) was added. The emission spectrum was recorded between 550 and 800 nm with an excitation wavelength of 526 nm for the ethidium bromide displacement experiment. The emission spectrum was recorded between 375 and 675 nm with an excitation wavelength of 358 nm for the DAPI displacement experiment. The fluorescence intensity at λ_{max} was used to determine the quenching constants of the platinum(II) complexes, **Pt-1a**, **Pt-2**, and **Pt-3**. The fluorescence studies were performed on a Varian Cary Eclipse spectrometer.

The quenching constant (K_q) was determined using the Stern-Volmer equation: $F^o/F = K_q[Q] + 1$, where F^o is the emission intensity of ct-DNA and ethidium bromide or DAPI in the absence of the platinum(II) complexes, **Pt-1a**, **Pt-2**, and **Pt-3**, F is the emission intensity in the presence of platinum(II) complexes, **Pt-1a**, **Pt-2**, and **Pt-3**, K_q is the quenching constant, and [Q] is the concentration of the platinum(II) complexes, **Pt-1a**, **Pt-2**, and **Pt-3**. The quenching constants were extrapolated from F^o/F versus [Q] plots.

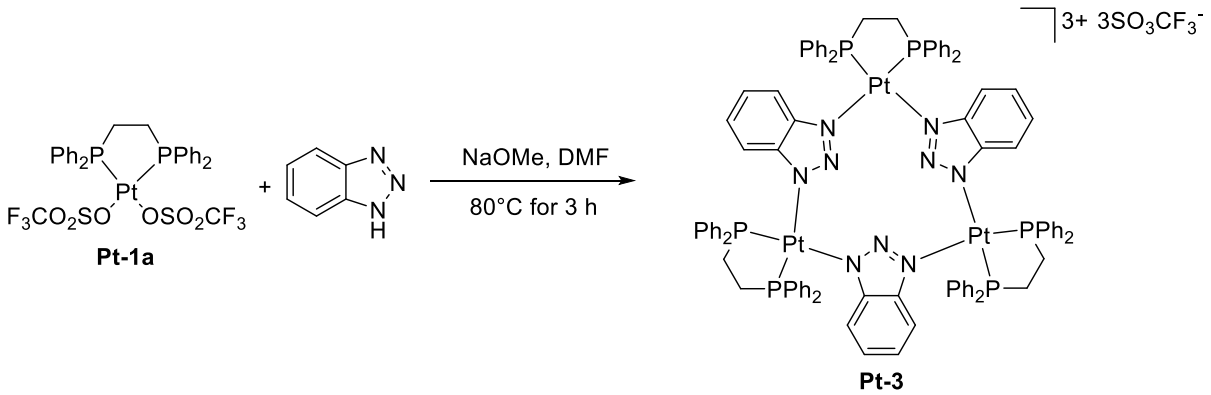

Scheme. S1 Chemical reaction scheme for the preparation of the tri-nuclear platinum(II) complex, **Pt-3**.

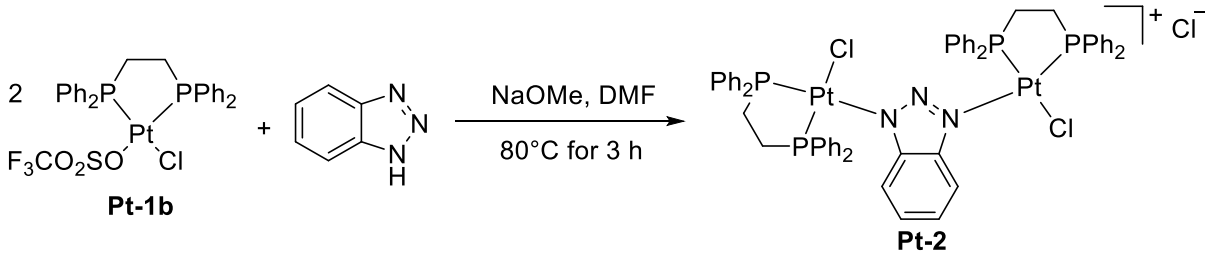

Scheme. S2 Chemical reaction scheme for the preparation of the di-nuclear platinum(II) complex, **Pt-2**.

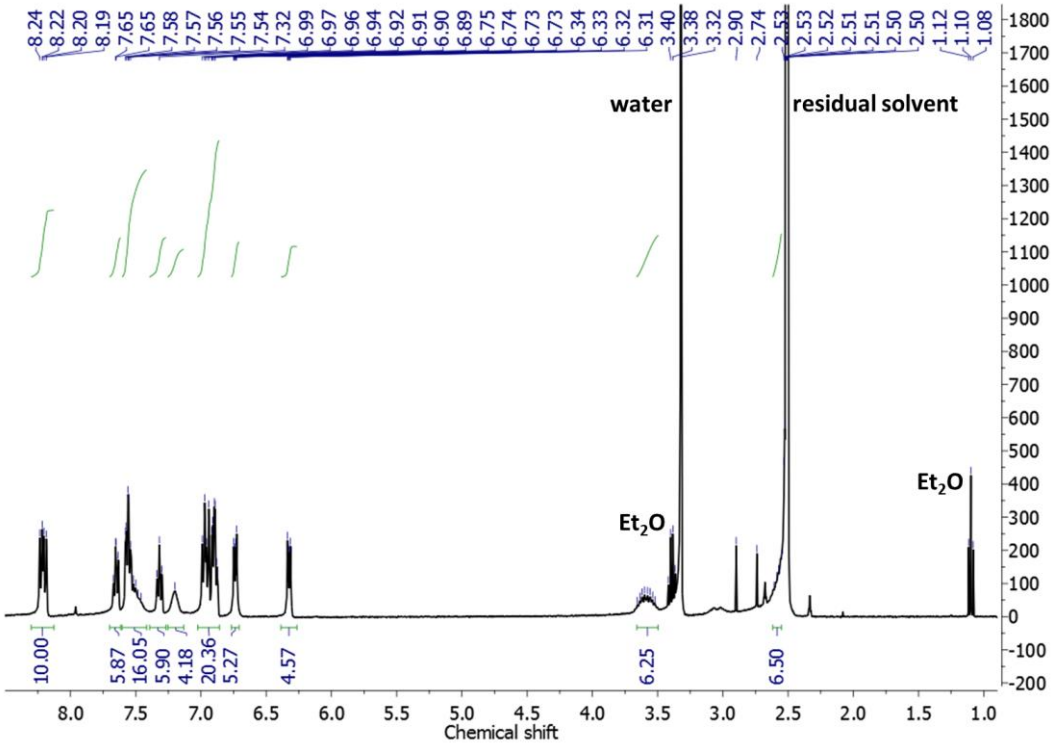

Figure. S1 ^{1}H NMR spectrum of **Pt-3** in DMSO-d_6.

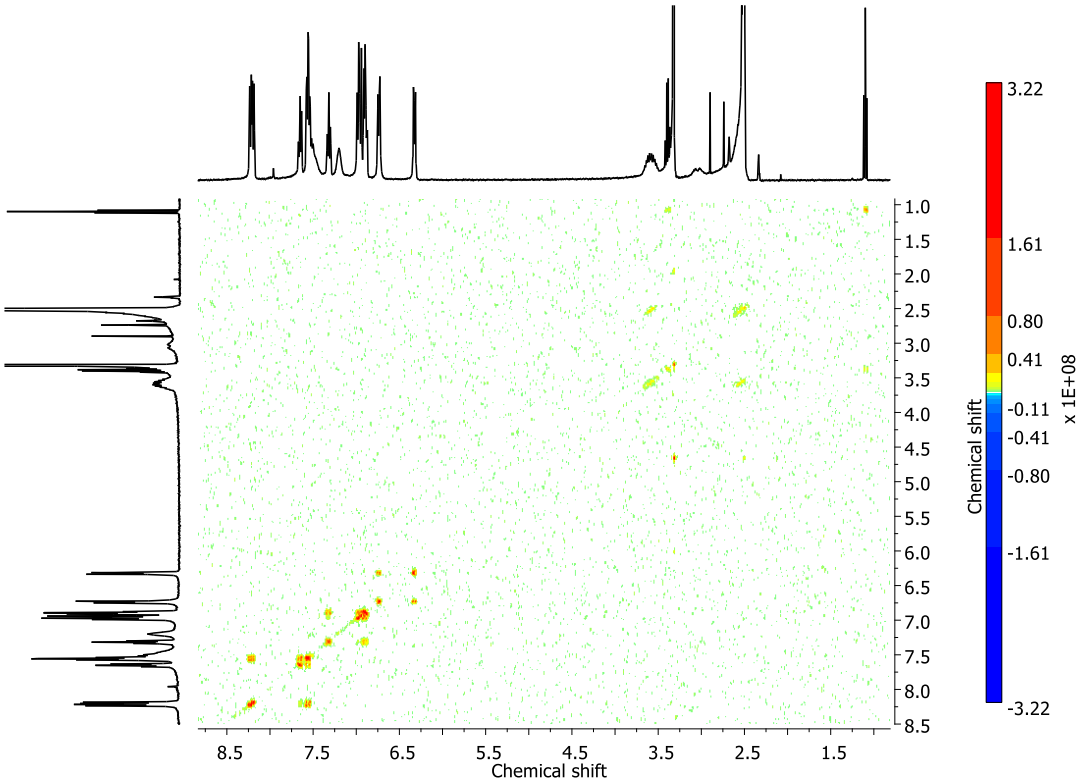

Figure. S2 ^{1}H-^{1}H COSY NMR spectrum of **Pt-3** in DMSO-d_6.

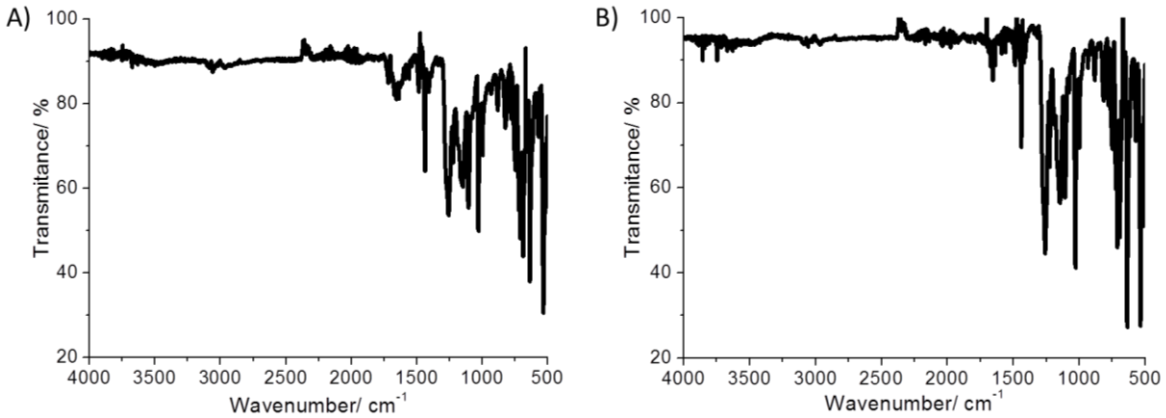

Figure. S3 IR spectrum of (A) **Pt-2** and (B) **Pt-3** in the solid form.

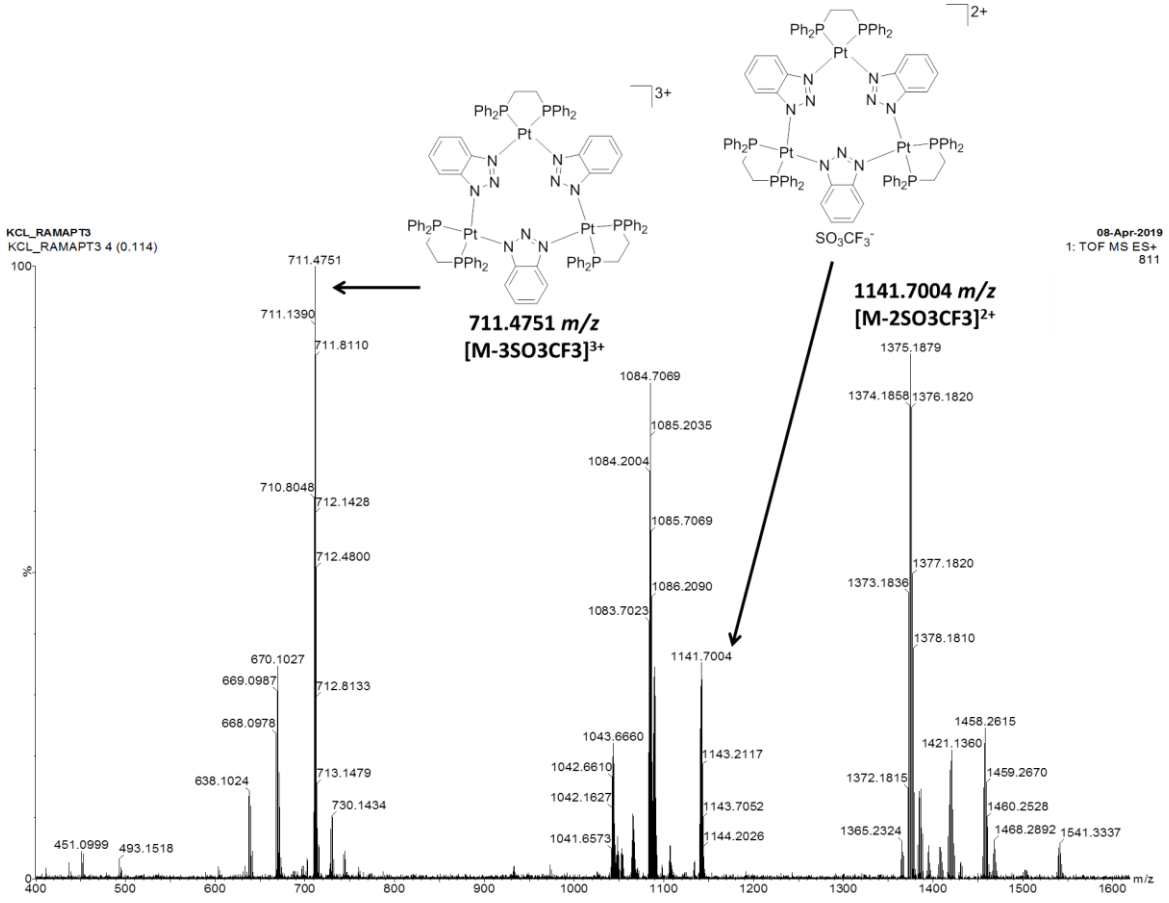

Figure S4. High resolution ESI mass spectrum (positive mode) of **Pt-3**.

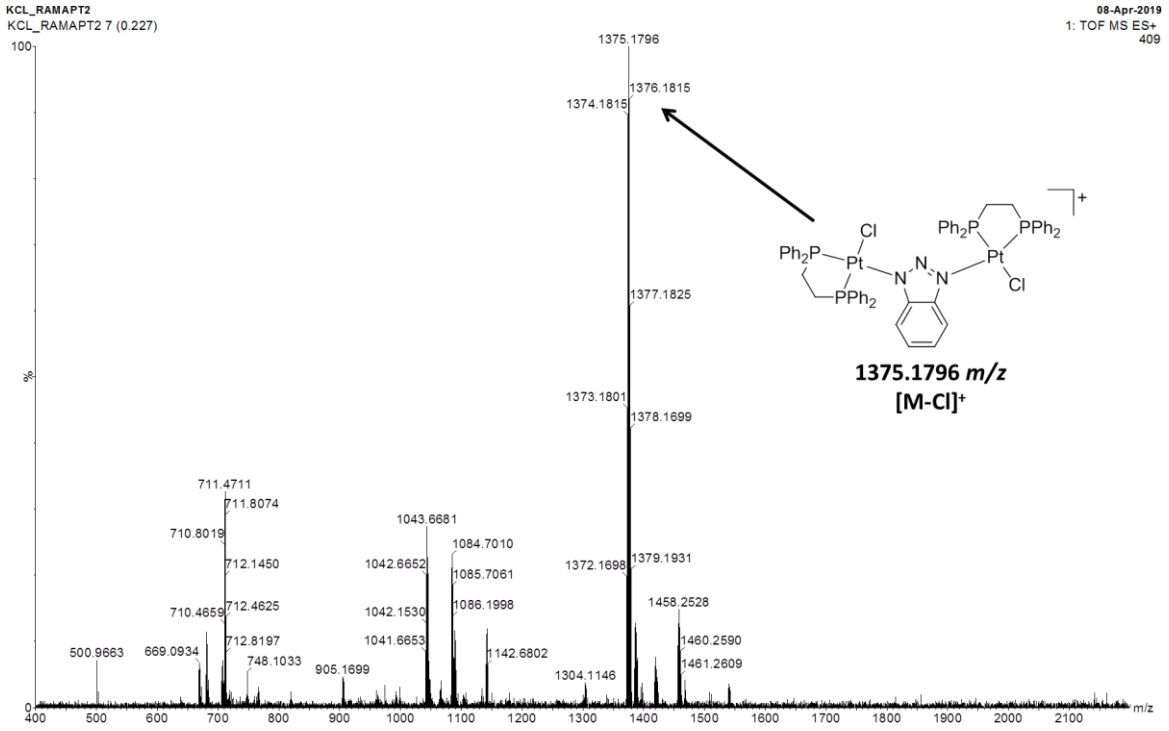

Figure S5. High resolution ESI mass spectrum (positive mode) of **Pt-2**.

Table S1. Crystallographic data of **Pt-3**•DMF and **Pt-2**.

Identification code	**Pt-3**•DMF (CCDC 1906805)	**Pt-2** (CCDC 1906803)
Empirical formula	$C_{102}H_{90}F_9N_{10}O_{10}P_6Pt_3S_3$	$C_{58}H_{52}Cl_3N_3P_4Pt_2$
Formula weight	2654.09	1411.43
Temperature	293(2) K	298(2) K
Wavelength	0.71073 Å	0.71073 Å
Crystal system	Triclinic	Orthorhombic
Space group	P -1	P 21 21 21
Unit cell dimensions	a = 15.2260(4) Å	a = 14.5186(6) Å
	b = 15.7912(3) Å	b = 15.3464(7) Å
	c = 22.9016(5) Å	c = 28.769(2) Å
	a = 97.626(2)°.	a = 90°.
	b = 99.962(2)°.	b = 90°.
	g = 99.769(2)°.	g = 90°.
Volume	5269.7(2) Å^3	6410.0(6) Å^3
Z	2	4

Density (calculated)	1.673 Mg/m^3	1.463 Mg/m^3
Absorption coefficient	4.200 mm^{-1}	4.620 mm^{-1}
F(000)	2610	2752
Crystal size	0.2 x 0.2 x 0.2 mm^3	0.2 x 0.2 x 0.2 mm^3
Theta range for data collection	2.963 to 28.853°.	2.395 to 25.028°.
Index ranges	-20<=h<=20, -21<=k<=20, -30<=l<=28	-17<=h<=10, -12<=k<=18, -16<=l<=34
Reflections collected	41976	16537
Independent reflections	22186 [R(int) = 0.0299]	10668 [R(int) = 0.0481]
Completeness to theta = 25.242°	98 %	99.8 %
Refinement method	Full-matrix least-squares on F^2	Full-matrix least-squares on F^2
Data / restraints / parameters	22186 / 0 / 1288	10668 / 108 / 607
Goodness-of-fit on F^2	1.054	0.999
Final R indices [I>2sigma(I)]	R1 = 0.0378, wR2 = 0.0820	R1 = 0.0627, wR2 = 0.1379
R indices (all data)	R1 = 0.0566, wR2 = 0.0918	R1 = 0.0979, wR2 = 0.1557
Absolute structure parameter	-	-0.034(8)
Largest diff. peak and hole	2.212 and -0.998 $e.Å^{-3}$	1.715 and -0.942 $e.Å^{-3}$

$R_1 = [\Sigma \, || F_0| - |F_c||/\Sigma|F_0|]$, $wR_2 = [\Sigma w(F_0^2 - F_c^2)^2/\Sigma w(F_0^2)^2]^{1/2}$

Table S2. Selected bond lengths (Å) and angles (°) for **Pt-3**•DMF.

Pt(1)-N(6)	2.080(4)	Pt(1)-N(7)	2.084(4)
Pt(1)-P(6)	2.2334(13)	Pt(1)-P(5)	2.2489(12)
Pt(2)-N(1)	2.073(4)	Pt(2)-N(4)	2.089(4)
Pt(2)-P(4)	2.2342(14)	Pt(2)-P(3)	2.2449(13)
Pt(3)-N(9)	2.077(4)	Pt(3)-N(2)	2.084(4)
Pt(3)-P(1)	2.2355(13)	Pt(3)-P(2)	2.2461(14)
N(6)-Pt(1)-N(7)	84.92(15)	N(6)-Pt(1)-P(6)	93.78(11)
N(7)-Pt(1)-P(6)	176.21(13)	N(6)-Pt(1)-P(5)	176.36(12)
N(7)-Pt(1)-P(5)	96.17(12)	P(6)-Pt(1)-P(5)	85.34(5)
N(1)-Pt(2)-N(4)	85.50(16)	N(1)-Pt(2)-P(4)	95.39(12)

N(4)-Pt(2)-P(4)	172.94(12)	N(1)-Pt(2)-P(3)	173.03(12)
N(4)-Pt(2)-P(3)	94.68(12)	P(4)-Pt(2)-P(3)	85.29(5)
N(9)-Pt(3)-N(2)	85.88(16)	N(9)-Pt(3)-P(1)	93.72(12)
N(2)-Pt(3)-P(1)	174.99(13)	N(9)-Pt(3)-P(2)	173.26(13)
N(2)-Pt(3)-P(2)	95.94(12)	P(1)-Pt(3)-P(2)	85.04(5)
C(60)-P(6)-Pt(1)	109.82(18)	C(47)-P(6)-Pt(1)	117.32(17)
C(210)-P(6)-Pt(1)	106.64(18)	C(57)-P(5)-Pt(1)	113.07(17)
C(211)-P(5)-Pt(1)	115.72(18)	C(43)-P(5)-Pt(1)	108.14(16)
C(37)-P(4)-Pt(2)	118.3(2)	C(214)-P(4)-Pt(2)	106.6(2)
C(29)-P(4)-Pt(2)	106.97(19)	C(18)-P(1)-Pt(3)	116.96(18)
C(270)-P(1)-Pt(3)	109.94(19)	C(16)-P(1)-Pt(3)	107.2(2)
C(34)-P(3)-Pt(2)	116.76(18)	C(31)-P(3)-Pt(2)	110.91(19)
C(28)-P(3)-Pt(2)	109.28(18)	C(23)-P(2)-Pt(3)	110.3(2)
C(21)-P(2)-Pt(3)	118.6(2)	C(15)-P(2)-Pt(3)	108.93(19)
N(5)-N(6)-Pt(1)	121.4(3)	C(68)-N(6)-Pt(1)	128.4(3)
N(5)-N(4)-Pt(2)	115.9(3)	C(200)-N(4)-Pt(2)	134.1(3)
N(3)-N(1)-Pt(2)	123.4(3)	C(222)-N(1)-Pt(2)	126.1(3)
N(8)-N(7)-Pt(1)	117.7(3)	C(202)-N(7)-Pt(1)	129.5(3)
N(3)-N(2)-Pt(3)	116.3(3)	C(12)-N(2)-Pt(3)	131.8(4)
N(8)-N(9)-Pt(3)	122.3(4)	C(69)-N(9)-Pt(3)	127.8(3)

Table S3. Selected bond lengths (Å) and angles (°) for **Pt-2**.

Pt(1)-N(1)	2.128(15)	Pt(1)-P(2)	2.234(5)
Pt(1)-P(1)	2.246(5)	Pt(1)-Cl(1)	2.350(5)
Pt(2)-N(3)	2.079(18)	Pt(2)-P(4)	2.226(6)
Pt(2)-P(3)	2.259(6)	Pt(2)-Cl(2)	2.348(6)
N(1)-Pt(1)-P(1)	92.7(4)	N(1)-Pt(1)-P(2)	178.2(4)
N(1)-Pt(1)-Cl(1)	90.0(4)	P(2)-Pt(1)-P(1)	85.7(2)
P(1)-Pt(1)-Cl(1)	177.2(2)	P(2)-Pt(1)-Cl(1)	91.6(2)
N(3)-Pt(2)-P(3)	179.4(5)	N(3)-Pt(2)-P(4)	94.1(5)
N(3)-Pt(2)-Cl(2)	87.9(5)	P(4)-Pt(2)-P(3)	85.6(2)
P(3)-Pt(2)-Cl(2)	92.4(2)	P(4)-Pt(2)-Cl(2)	177.3(2)
C(7)-P(1)-Pt(1)	116.2(8)	C(1)-P(1)-Pt(1)	110.3(6)
C(47)-P(4)-Pt(2)	118.3(6)	C(13)-P(1)-Pt(1)	108.8(7)
C(41)-P(4)-Pt(2)	110.8(6)	C(40)-P(4)-Pt(2)	107.7(8)
C(39)-P(3)-Pt(2)	107.0(8)	C(27)-P(3)-Pt(2)	115.5(8)

C(21)-P(2)-Pt(1)	111.4(7)	C(33)-P(3)-Pt(2)	115.5(7)
C(15)-P(2)-Pt(1)	118.6(7)	C(14)-P(2)-Pt(1)	108.9(8)
C(54)-N(1)-Pt(1)	127.2(14)	N(2)-N(1)-Pt(1)	120.4(11)
C(53)-N(3)-Pt(2)	132.9(13)	N(2)-N(3)-Pt(2)	119.9(12)

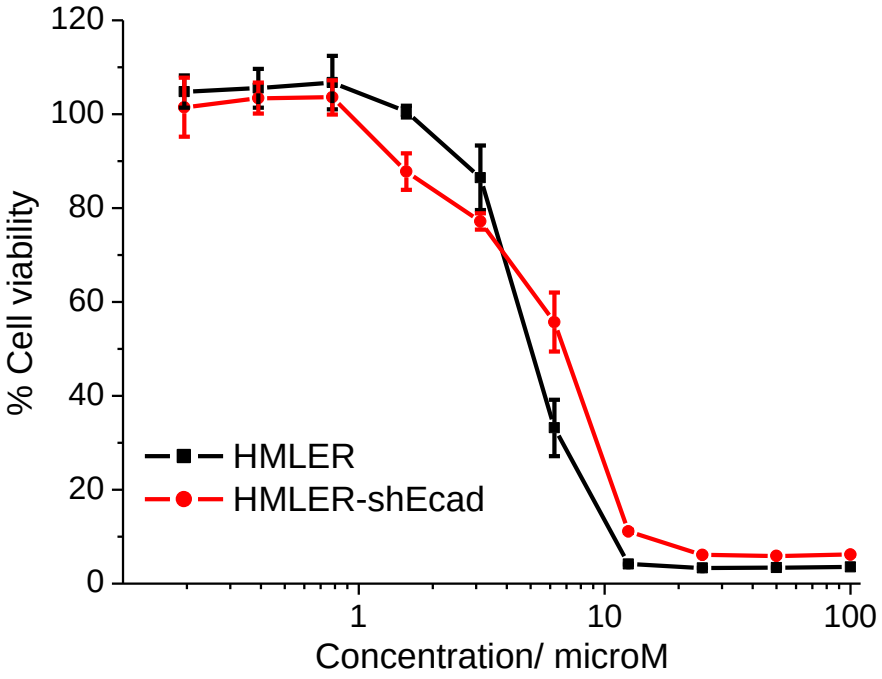

Figure S6. Representative dose-response curves for the treatment of HMLER and HMLER-shEcad cells with **Pt-1a** after 72 h incubation.

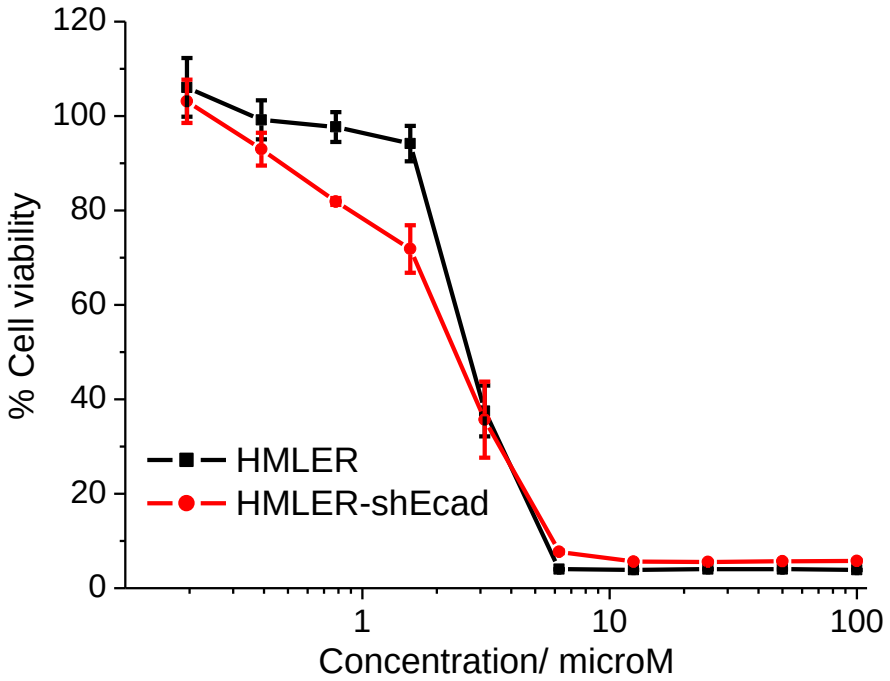

Figure S7. Representative dose-response curves for the treatment of HMLER and HMLER-shEcad cells with **Pt-2** after 72 h incubation.

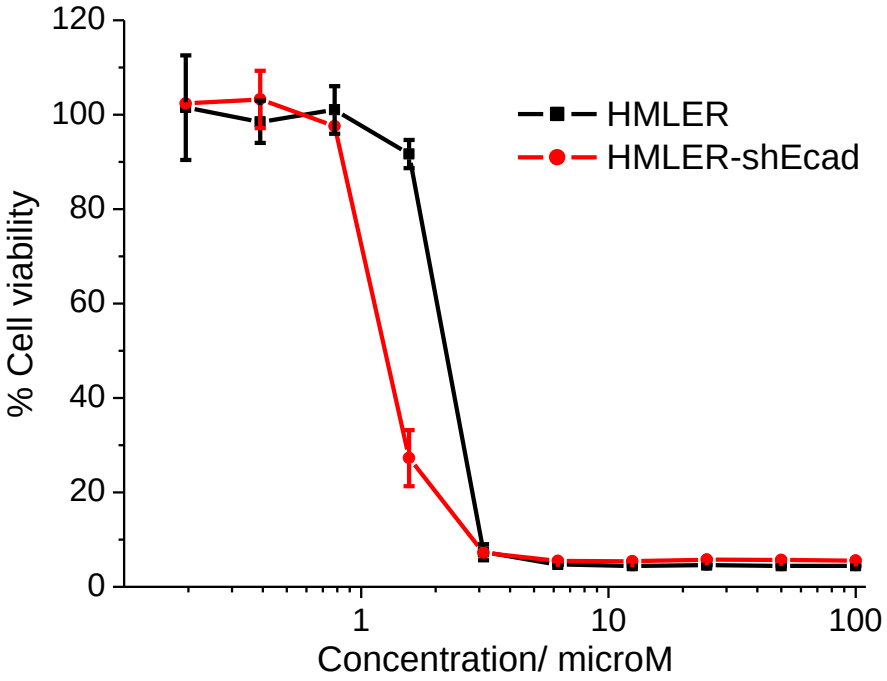

Figure S8. Representative dose-response curves for the treatment of HMLER and HMLER-shEcad cells with **Pt-3** after 72 h incubation.

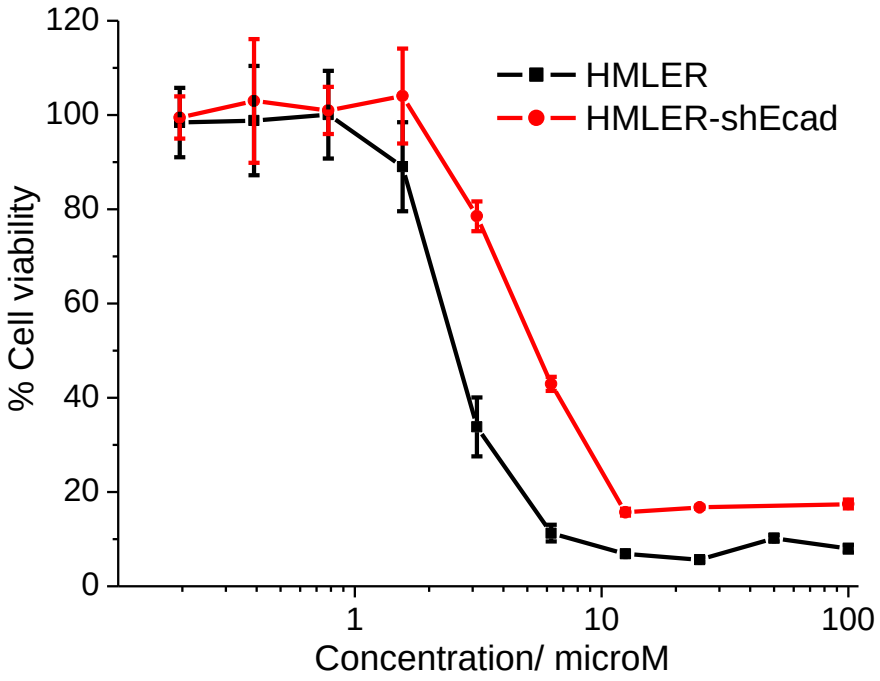

Figure S9. Representative dose-response curves for the treatment of HMLER and HMLER-shEcad cells with cisplatin after 72 h incubation.

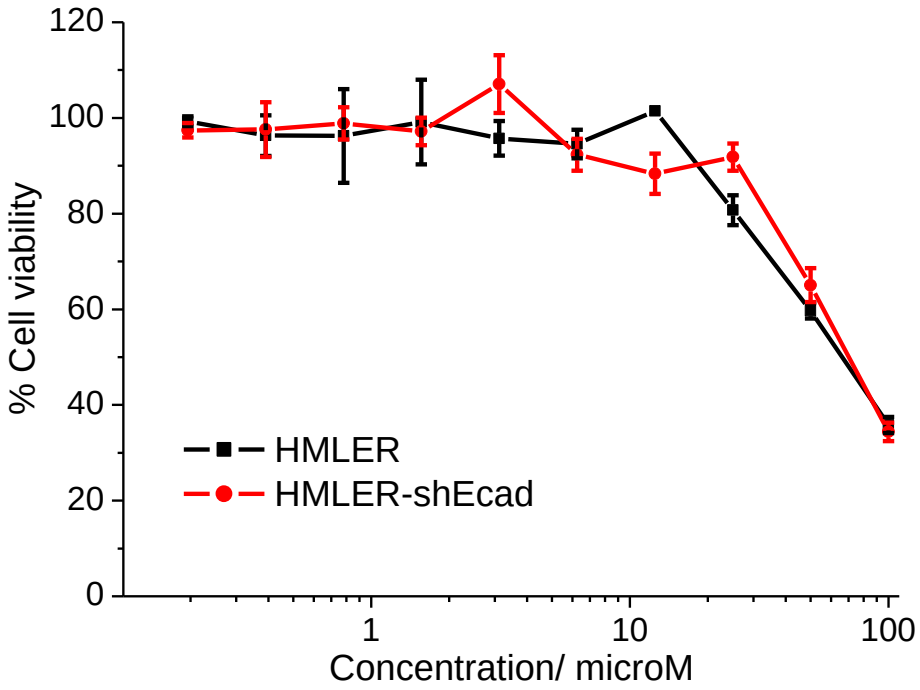

Figure S10. Representative dose-response curves for the treatment of HMLER and HMLER-shEcad cells with carboplatin after 72 h incubation.

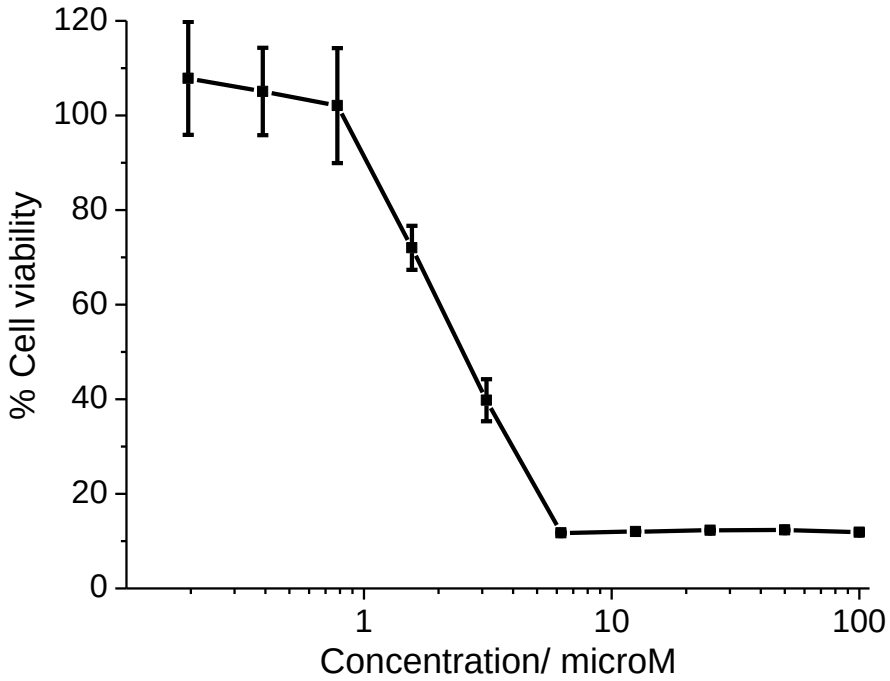

Figure S11. Representative dose-response curves for the treatment of MCF10A cells with **Pt-3** after 72 h incubation.

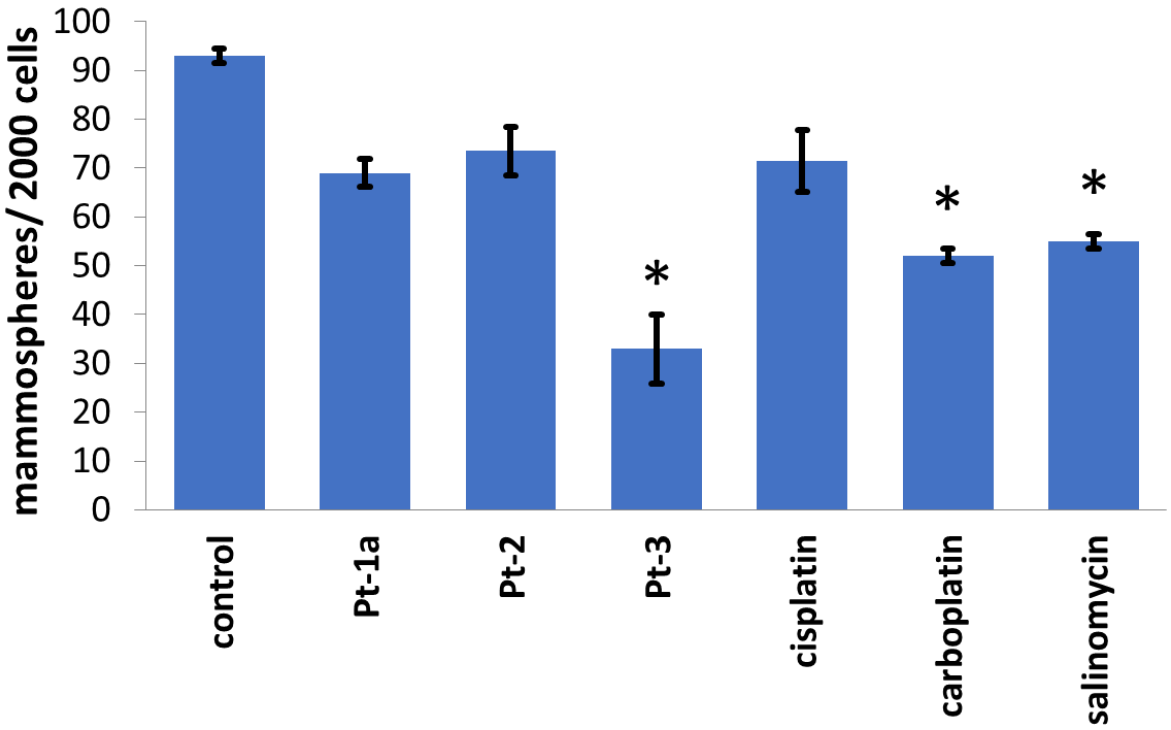

Figure S12. Quantification of spheroid formation with HMLER-shEcad cells untreated and treated with **Pt-1a**, **Pt-2**, **Pt-3**, cisplatin, carboplatin, and salinomycin at their respective IC_{20} values for 5 days. Error bars = SD and Student *t-test*, * = $p < 0.05$.

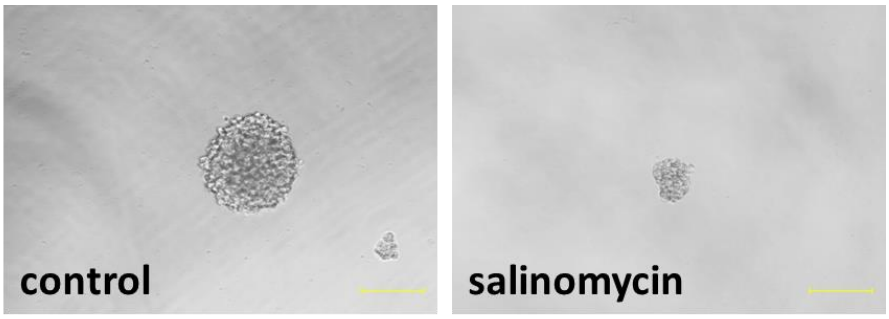

Figure S13. Representative bright-field images (× 20) of HMLER-shEcad spheroids in the absence and presence of salinomycin at its IC_{20} value (5 days incubation).

Table S4. Experimentally determined LogP values for **Pt-2**, **Pt-3**, and cisplatin.

Platinum complex	LogP
Pt-2	-0.27
Pt-3	0.32
cisplatin[a]	-2.21

[a] Reported in reference 3.

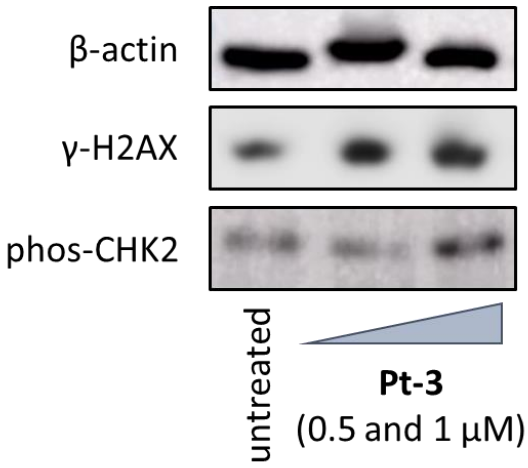

Figure S14. Immunoblotting analysis of proteins related to the DNA damage pathway. Protein expression in HMLER-shEcad cells following treatment with **Pt-3** (0.5 and 1 μM for 72 h).

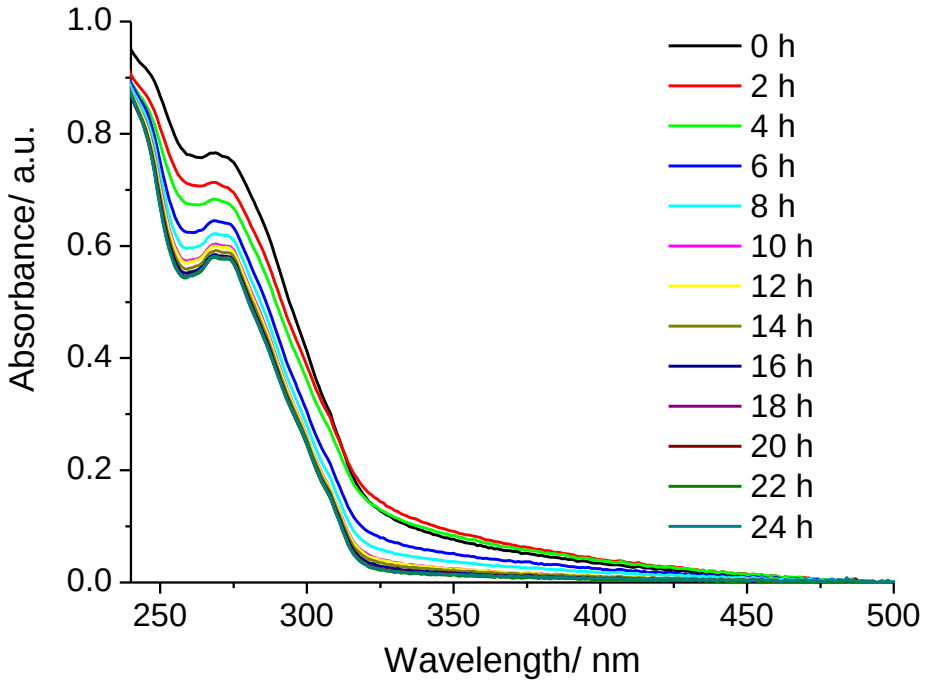

Figure S15. UV-Vis spectrum of **Pt-3** (25 μM) in PBS:DMSO (200:1) over the course of 24 h at 37 ºC.

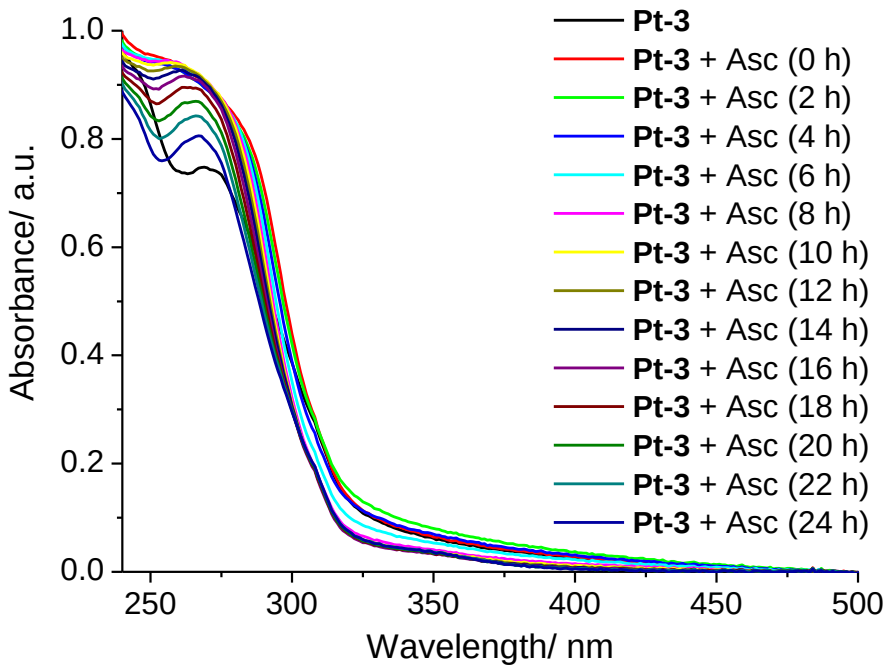

Figure S16. UV-Vis spectrum of **Pt-3** (25 μM) in the presence of ascorbic acid (250 μM) in PBS:DMSO (200:1) over the course of 24 h at 37 °C.

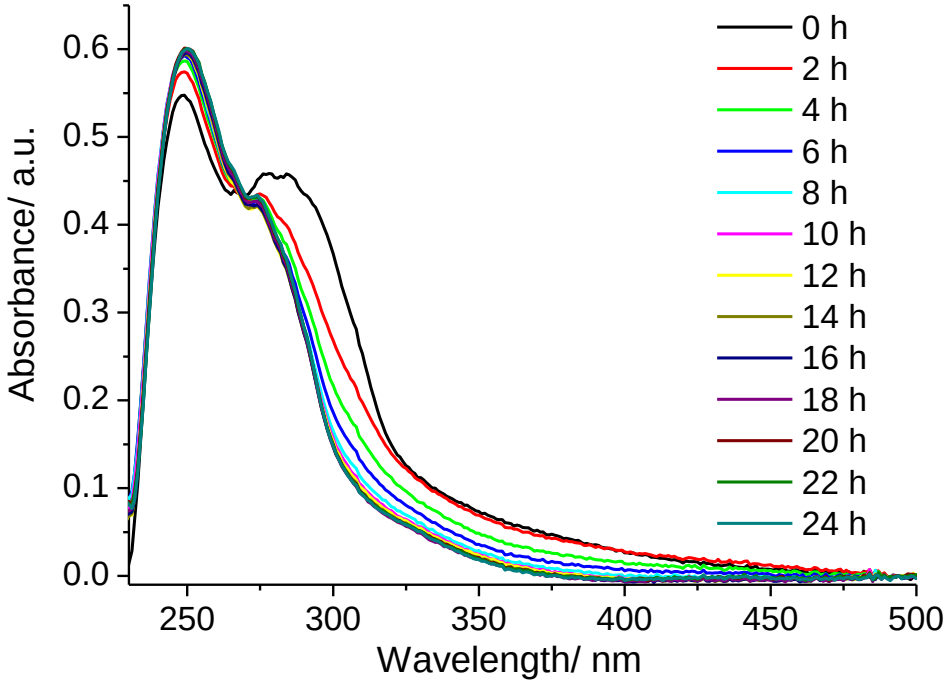

Figure S17. UV-Vis spectrum of **Pt-3** (25 μM) in mammary epithelial cell growth medium (MEGM):DMSO (200:1) over the course of 24 h at 37 °C.

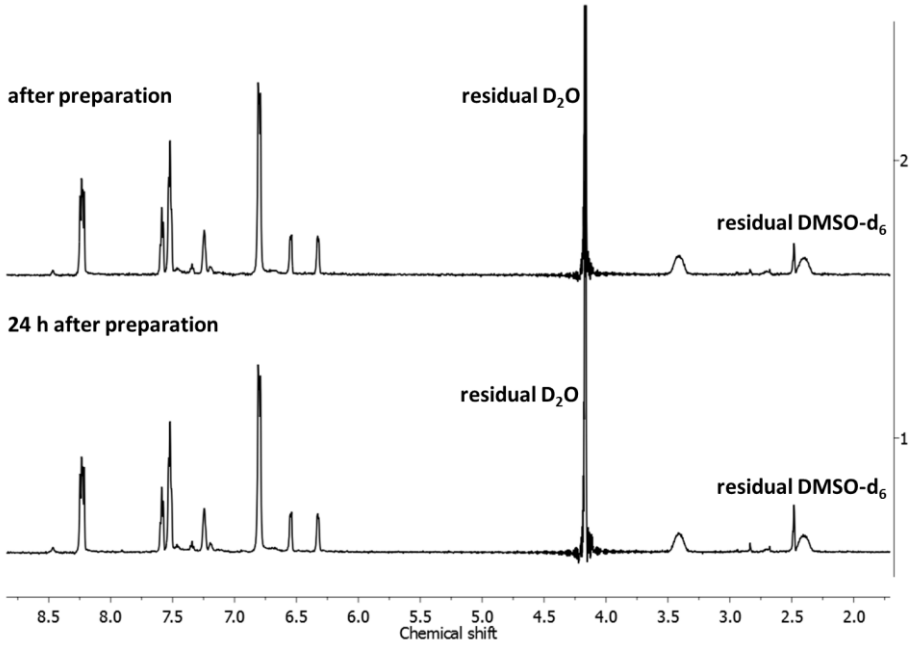

Figure S18. ^{1}H NMR spectra of **Pt-3** in DMSO-d_6:D_2O (1:1) after preparation (top spectrum) and after 24 h incubation at 37 ^oC (bottom spectrum).

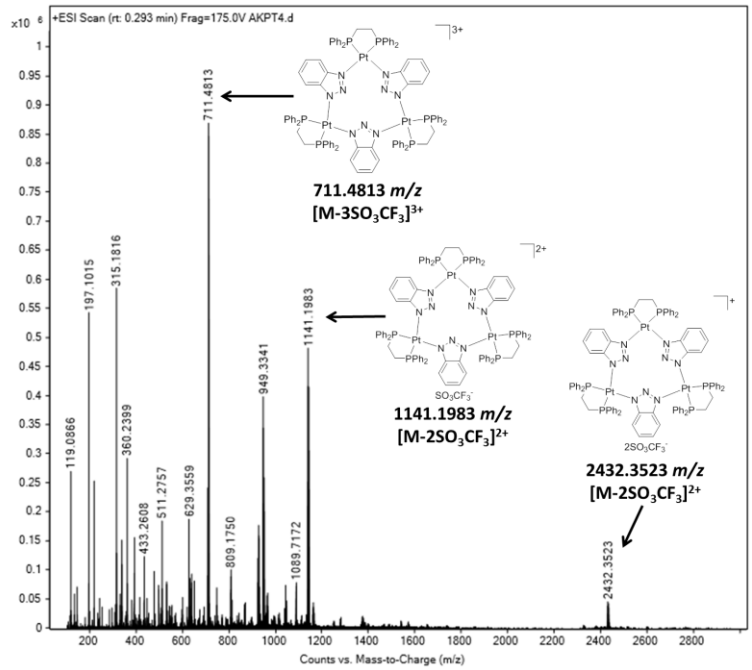

Figure S19. ESI mass spectrum (positive mode) of **Pt-3** in DMSO:D_2O after 24 h incubation at 37 ^oC.

Discussion of data presented in Figure S18-19. Upon incubation of **Pt-3** in DMSO-d_6:D_2O (1:1) for 24 h at 37 ^oC, there was no observable changes in the ^{1}H NMR spectrum, indicating stability (Figure S18). Peaks corresponding to [**Pt-3**-SO_3CF_3]$^+$ (2432.3523 m/z), [**Pt-3**-$2SO_3CF_3$]$^{2+}$ (1141.1983 m/z), and [**Pt-3**-$3SO_3CF_3$]$^{3+}$ (711.4813 m/z) with the appropriate isotopic distribution were observed in the positive mode of the ESI mass spectrum (Figure S19), further proving that **Pt-3** remains fully intact under these conditions.

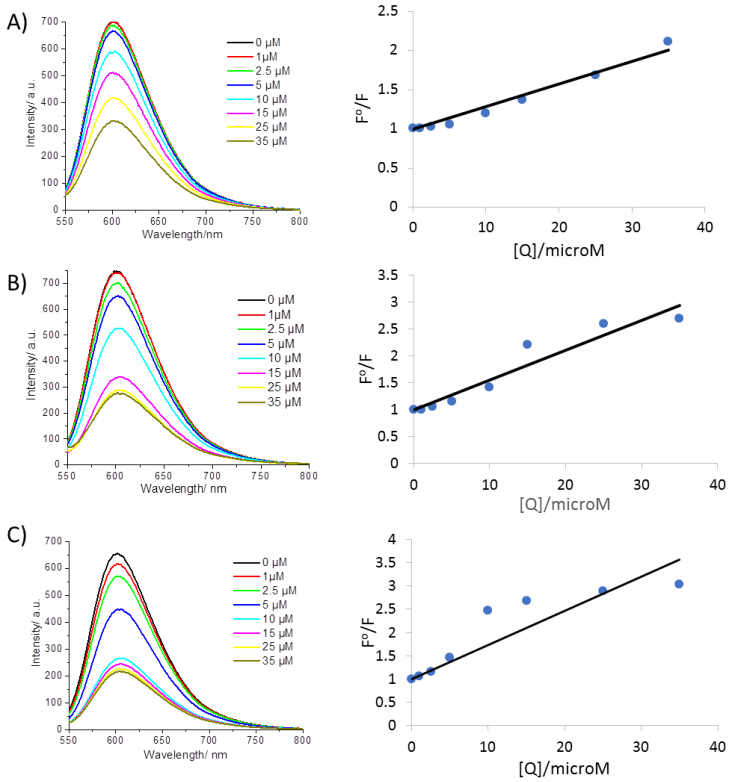

Figure S20. Emission spectra for ethidium bromide (1 μM) bound to ct-DNA (1:20 ratio) upon addition of aliquots of **Pt-1a**, **Pt-2**, and **Pt-3** (A-C) and the corresponding F°/F versus [Q] plots for **Pt-1a**, **Pt-2**, and **Pt-3** (A-C).

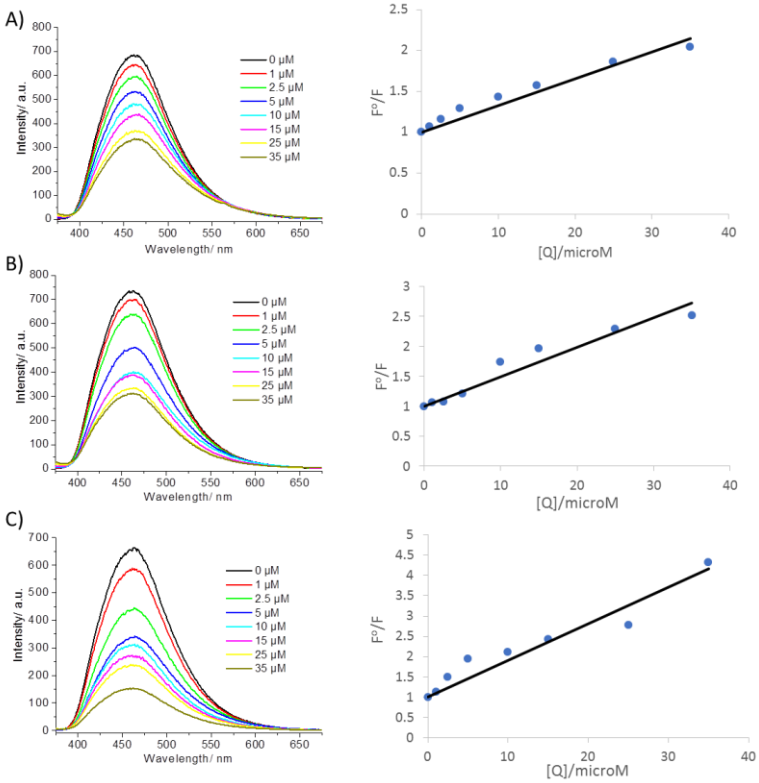

Figure S21. Emission spectra for DAPI (1 μM) bound to ct-DNA (1:20 ratio) upon addition of aliquots of **Pt-1a**, **Pt-2**, and **Pt-3** (A-C) and the corresponding F°/F versus [Q] plots for **Pt-1a**, **Pt-2**, and **Pt-3** (A-C).

Table S5. Ethidium bromide and DAPI quenching constants (K_q) for the interaction of **Pt-1a**, **Pt-2**, and **Pt-3** (0-35 μM) with ct-DNA (20 μM).

Pt(II) complex	Ethidium bromide K_q/ M^{-1}	DAPI K_q/ M^{-1}
Pt-1a	$2.48 \pm 0.56 \times 10^4$	$2.85 \pm 0.62 \times 10^4$
Pt-2	$6.11 \pm 0.81 \times 10^4$	$4.77 \pm 0.21 \times 10^4$
Pt-3	$7.35 \pm 0.06 \times 10^4$	$7.64 \pm 0.20 \times 10^4$

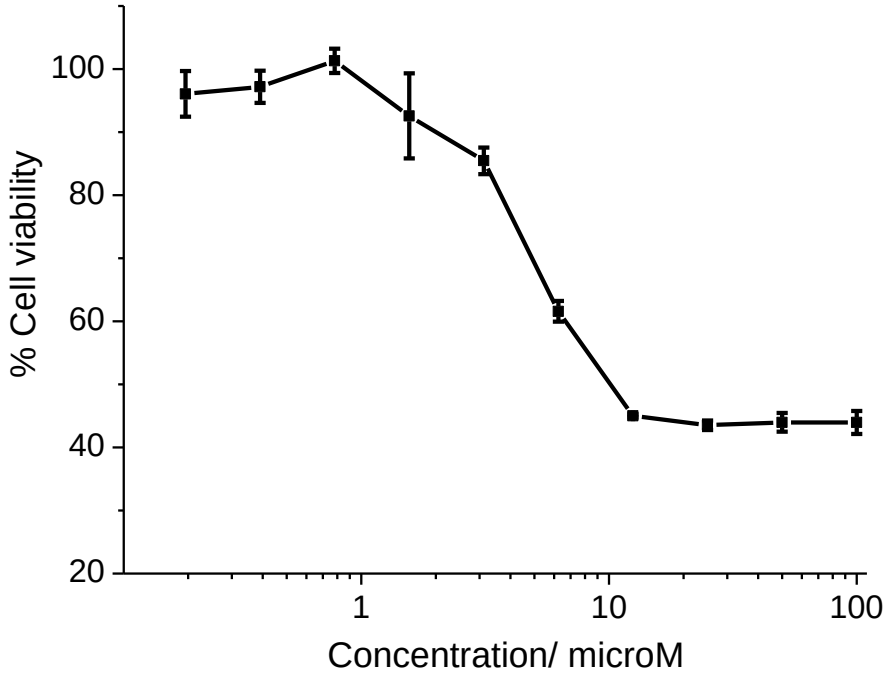

Figure S22. Representative dose-response curves of cisplatin against HMLER-shEcad cells in the presence of z-VAD-FMK (5 μM) after 72 h incubation.

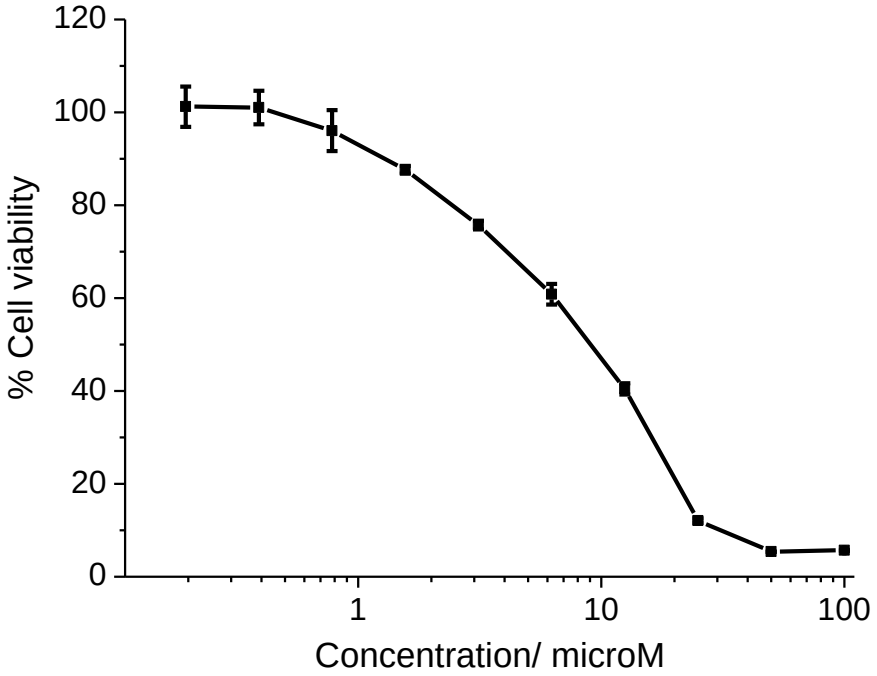

Figure S23. Representative dose-response curves of **Pt-1** against HMLER-shEcad cells in the presence of z-VAD-FMK (5 μM) after 72 h incubation.

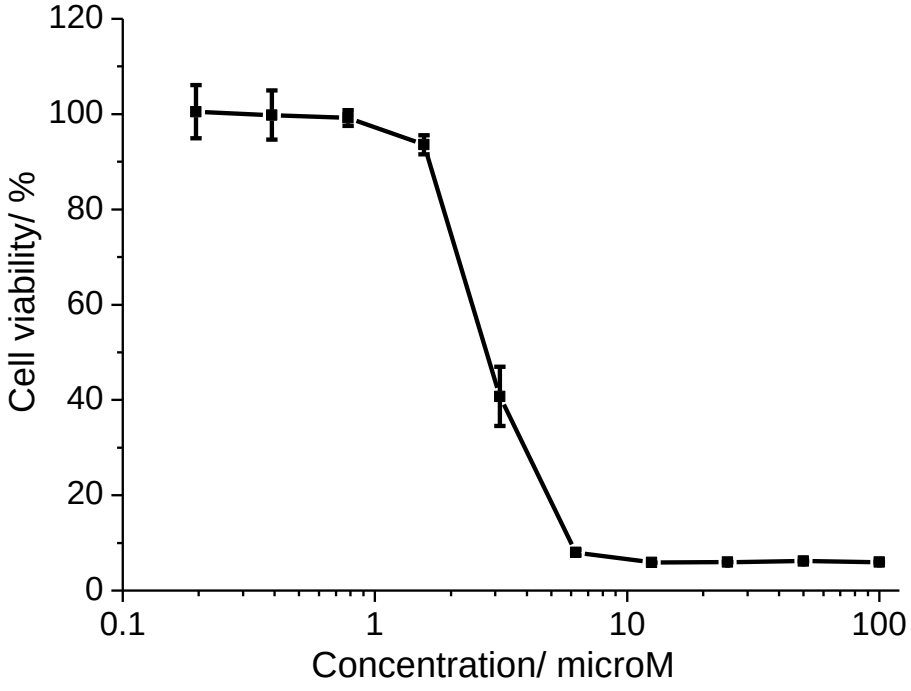

Figure S24. Representative dose-response curves of **Pt-2** against HMLER-shEcad cells in the presence of z-VAD-FMK (5 μM) after 72 h incubation.

References

[1] a) G. S. Hill, G. P. A. Yap, R. J. Puddephatt, *Organometallics* **1999**, *18*, 1408-1418; b) F. E. Hahn, D. Klusmann, T. Pape, *Eur. J. Inorg. Chem.* **2008**, *2008*, 4420-4424.

[2] G. Sheldrick, *Acta Cryst.* **2008**, *A64*, 112-122.

[3] J. J. Wilson, S. J. Lippard, *J. Med. Chem.* **2012**, *55*, 5326–5336.